Developing a high frequency current amplifier for Scanning Tunnelling Microscopy.

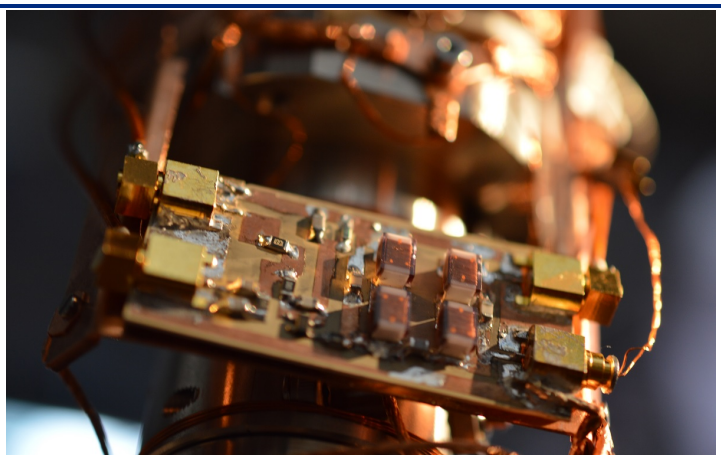

THESIS

submitted in partial fulfillment of the
requirements for the degree of

BACHELOR OF SCIENCE
in
PHYSICS

Author :	Tjerk Benschop
Student ID :	1406035
Supervisor :	Dr. M.P. Allan
2^{nd} corrector :	Prof. Dr. J.M. van Ruitenbeek

Leiden, The Netherlands, August 9, 2016

Developing a high frequency current amplifier for Scanning Tunnelling Microscopy.

Tjerk Benschop

Huygens-Kamerlingh Onnes Laboratory, Leiden University
P.O. Box 9500, 2300 RA Leiden, The Netherlands

August 9, 2016

Abstract

Scanning Tunnelling Microscopy (STM) is a well established and widely used technique in the world of surface physics, capable of measuring atomic resolution topographs within seconds. There are however still improvements we can make. Where spatial resolution is almost perfect, the temporal resolution of STM is quite terrible, limiting the measurement of rapid fluctuations in the tunnelling current. This withholds STM from for example measuring shotnoise and single atom spin relaxation. We try to solve this issue by designing a small cryogenic amplifier and implementing it close to the tip of a STM setup, increasing its bandwidth around 2.8MHz. We discus simulations as well as test results from our amplifier. Finally, we give an outlook on how to improve this design in order to measure shotnoise.
keywords: shotnoise, high frequency STM, Rf STM, scanning tunnelling microscopy, cryogenic amplifier, resonator, tank circuit.

Contents

Chapter 1

Introduction

The first Scanning Tunnelling Microscope (STM) was built in 1982 [1]. Since then, it has been optimized in many ways. Advanced mass spring systems to dampen external vibration that could potentially harm the measurement, better vacuum technology resulting in less pollution of the tunnelling junction, etc. Good STM setups nowadays can easily measure atomic resolution topographs in just a matter of seconds. Furthermore, they can be used to do scanning tunnelling spectroscopy; a technique that measures $\frac{dI}{dV}$, giving direct insight in the local density of states of electrons in a sample. Really unique about this is that contrary to other surface spectroscopy techniques, the tunnelling current from a STM only flows from a surface as large as a few $Å^2$, which translates to a very high spatial accuracy.
There are however still points that can be improved upon. In this thesis, we will address the temporal resolution of STM: Even the best setups can only measure fluctuations of at best a couple of hundreds of Hz due to the way fundamental STM circuitry is arranged. Therefore, detecting fast changes in the tunnelling current, which is already a small signal in itself, is virtually impossible. This limits STM from for example measuring spin relaxation with atomic resolution. There are ways to work around this, still allowing for the measurement of single spin relaxation [2], but until now, there are no STM setups that can directly measure it due to the lack of bandwidth.
This thesis will be centered around the measurement of shotnoise: fluctuations in the tunnelling current due to the quantization of charge. Currently, this is impossible due to the issue with temporal resolution. Still, we would like to be able to measure this shotnoise from the tunnelling current of our STM. An application of this could be shotnoisemeasurements

on cuprates. Cuprates are compounds of copper and oxygen which have high T_c superconducting properties. Currently, STM is unable to locate the position of dopant atoms in those cuprate samples. Because we expect shotnoise to be influenced by the sample [3], measuring shotnoise at different points on the sample could give us insight in where the dopants are located. Another reason is local thermometry: since shotnoise is dependent on the temperature, one could determine this very locally by measuring a shotnoisecurve at a certain point on a sample.
To conclude the introduction, we have to address why we want to measure shotnoise around 2.8MHz. The reason for this lies with what we call 1/f noise: Due to random motion of impurities in conductors, its conductance fluctuates and becomes dependent on time. As the name suggest, this noise falls of as 1/f. Hence, we want to measure at 2.8Mhz, where the shotnoise dominates over the 1/f noise (figure 1.1). Furthermore, at this frequency, noise due to vibrations of the STM setup itself will be minimal.

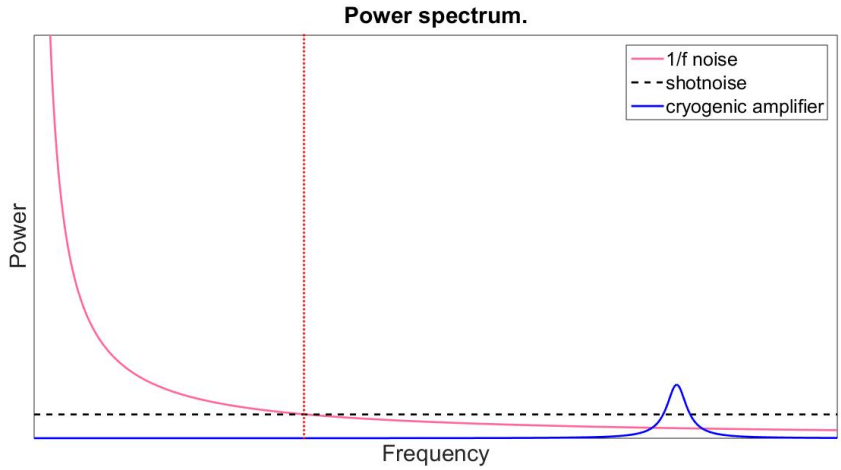

Figure 1.1: *Representation of the power spectrum of the tunnelling current. At lower frequencies, the spectrum is dominated by 1/f noise (left of the red line), forcing shotnoise measurements to be conducted at higher frequencies.*

We present a design for a cryogenic amplifier, close to the tip of a STM setup, which creates a band pass filter around a predefined frequency (our design is tuned to 2.8MHz). We discuss simulations, as well as test results of this amplifier.

Chapter 2

Theory

2.1 Standard STM circuitry

STM is a technique that is based on measuring the tunnelling current from a biased junction between a scanning tip and a sample. Since this current is proportional to the distance between tip and sample, measuring this gives insight in the topology of the surface of the sample. There are two ways this can be executed:

- Constant height mode: while scanning, the distance between the tip and sample is kept fixed. An increase/decrease in tunnelling current means that the sample is higher/lower in that area. A big disadvantage of this is that the tip is quite prone to crashing: if the set tip distance is smaller than the maximum height difference in the sample, the tip automatically runs in the sample while scanning.
- Constant current mode: Here, the tunnelling current is kept constant by measuring it and putting it into a feedback loop that adjust the junction resistance (distance between tip and sample). By reading out the feedback a topograph can be constructed: if the sample is higher/lower at some point, the feedback loop will retract/detract the tip a bit, keeping the tunnelling current constant. This method is preferred, since it is less prone to crashing and since this is the only mode in which scanning tunnelling spectroscopy can be performed.

In order to do measure the tunnelling current, most STM setups resort to the circuitry displayed in figure 2.1.
A bias voltage is applied between the sample and the tip, in order to generate a net current. This current travel through a coaxial cable (usually out

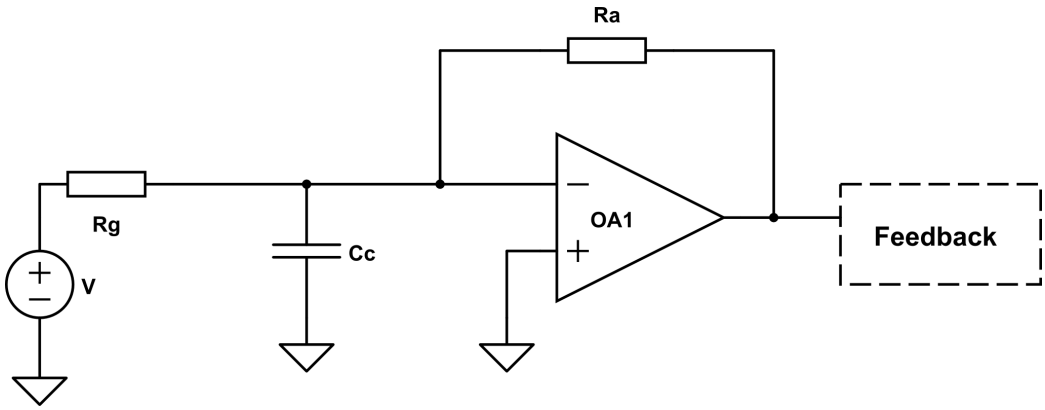

Figure 2.1: *Schematic overview of default STM circuitry. R_g is a resistor, modelling the tunnel junction between tip and sample. C_c is a parasitic capacitance to ground due to the cable that connects the tip to an IV converter.*

of a cryogenic environment), to an IV converter: an Operational Amplifier (OpAmp) with a big, often modifiable, resistor parallel to it. This IV converter does exactly what the name suggests: it converts a current into a voltage, proportional to a certain gain. In the circuit from figure 2.1, this gain is equal to -R_a:
Assuming we are dealing with an ideal OpAmp, the voltage at the positive input equals the voltage at the negative input:

$$V_+ = V_- = 0$$

If we then calculate the output voltage of the OpAmp:

$$V_{out} = g * (V_+ - V_-) = 0 = -I_{in} * R_a$$

Here, g is the gain of the OpAmp itself. If we then calculate the transfer function of this IV converter:

$$\frac{V_{out}}{I_{in}} = \frac{-I_{in} * R_a}{I_{in}} = -R_a$$

Typically, we do STM with a tunnel junction of the order of 1GΩ or larger. This means that the tunnelling current will be in the order of pA to nA. To measure this, we require a gain of 10^6 or larger, which can be achieved by choosing R_a as 1MΩ or bigger.
Up until this point, we left one element out of the picture, because the tunnelling current is a(n) (almost) DC signal making it unimportant, but as soon as we start thinking about fluctuations in this tunnelling current, we

need to take the capacitance of the tip cable into account (C_c) (figure 2.1). For AC signals, the impedance of this parasitic capacitance becomes finite, which means that the circuit loses signal to ground. We simulated this in figure 2.2;

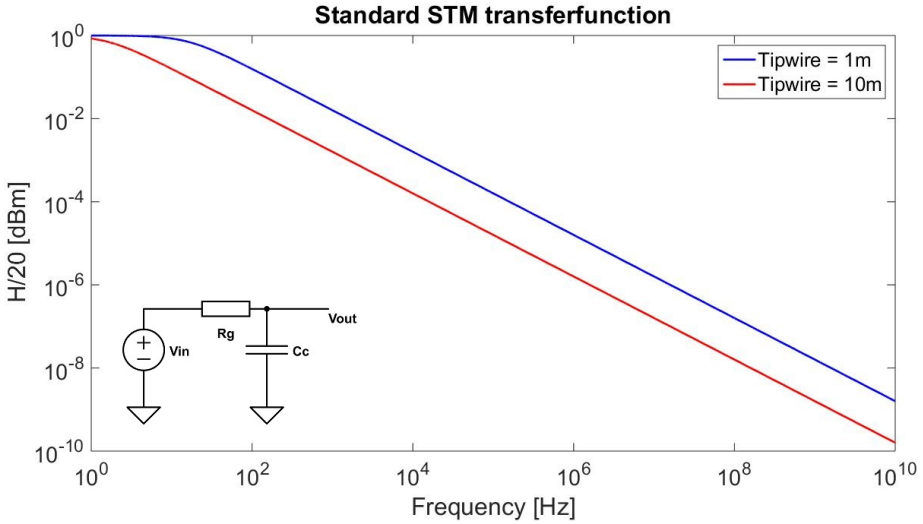

Figure 2.2: *Transfer function of a tunnel junction (R_g = 0.1GΩ) connected via a coax cable (C_c, 100 pF/m) to an external device. As you can see from the figure, even in the most favourable case, the cutoff frequency of the ensemble lies around 100Hz.*

The figure shows that even in the most optimistic scenario, the cutoff frequency of STM electronics is a couple of hundred hertz. This means that measuring small signals ($\leq$ nW/Hz) beyond that frequency is virtually impossible.

2.2 High Electron Mobility Transistor

There are multiple solutions to overcome this issue. One can for example compensate for the cable capacitance in order to extend the bandwidth of the circuit [4], however, instead of doing this, we propose to move the bandwidth by designing a cryogenic amplifier close to the tip. In this way, the signal we want to measure, which in our case will be shotnoise, will be amplified before going through the tip cable. A big advantage of this is that we can do measurements at virtually any frequency we want, as long as we tailor the amplifier to it, whereas extending bandwidth can only be done up to a certain frequency.

The amplifier we built makes use of a Hemt, or High electron mobility transistor, which is basically a field effect transistor (FET). The main difference between them is that where a FET is made up out of layers of differently doped materials (NPN- or PNP junction), a Hemt is made up out of 2 materials with different band gaps. Whereas in a FET, the charge carriers come forth from the dopants, in a Hemt, the carriers come from one of the 2 material, (usually strongly n-doped), which acts as a donor layer. From there, they drop completely in the undoped layer, forming a 2DEG. Since there are no dopants in this layer, the electrons cannot collide into them, causing the formed conduction channel to have very low resistivity: Ballistic transport occurs (contrary to a channel formed in a normal FET).

2.3 Shotnoise

The first test for our amplifier will be to measure shotnoise on different samples. Shotnoise are the fluctuations in current due to the quantization of charge. One can classically think about this in the following way: in the macroscopic world, a current is somewhat similar to a flowing tap: a constant stream of water is pouring out (assuming the plumber did its job properly). What we observe is just a constant flow, but if we look at this flow microscopically, we see that the water flow is made up out of a constant stream of water molecules. In case of our electric current, this could be the individual electrons. Should we have access to a super fast, super good detector, we could even measure the incoming electrons as single events: at a certain point in time, an electron enters the detector, then after a certain time, another one and another one and so on. What's important to realize is that the time between those detection events is not constant. Still, in our macroscopic world, we just speak about 'a' current. With this, we address the average amount of particles measured in time. Fluctuations from this average current are what we call shotnoise.
If we regard the electrons in the current as randomly and independently emitted, we can describe them with poissonian statistics. The spectral density of the fluctuations would then be:

$$S = 2e\bar{I},$$

where e is the elementary charge and $\bar{I}$ is the mean current. The factor 2 is due to the fact that positive and negative frequencies contribute equally.
However, we can do better than that. The current noise of the junction is

given by [5]:

$$S = \frac{2}{R}\int [f_t(E)(1-f_s(E)) + f_s(E)(1-f_t(E))]dE$$

Here, R is the resistance of the junction and f_t, f_s are the Fermi-Dirac distributions of the tip and sample respectively:

$$f_i = \frac{1}{e^{\frac{E-\mu_i}{k_b T}} + 1}$$

, where μ_i is the chemical potential of the tip/sample, k_b is the Boltzmann constant and T is the temperature. If we put a bias, V, over our junction, $\mu_s - \mu_t \approx eV$ and the integral can be evaluated to obtain:

$$S = 2e\frac{V}{R}\coth\left(\frac{eV}{2k_bT}\right)$$

We can plot this result for different temperatures (figure 2.3).

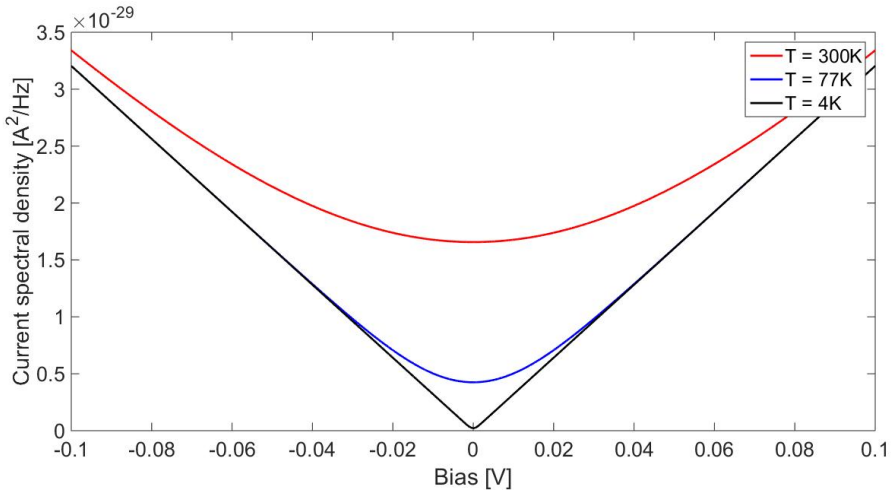

Figure 2.3: *Plot of the power spectral density of shotnoise as function of bias voltage for different temperatures. R was chosen to be 1GΩ.*

Since V and R are just measurement parameters, measuring the shotnoise and fitting this result can give us a way to indirectly measure the local temperature.

Chapter 3

Methods and Materials

To increase the temporal resolution of a STM setup, we designed a cryogenic amplifier close to the tip, based on Di Carlo et al. [6] and Arakawa et al. [7] in order to make shotnoise measurements possible. In this part, we discuss the different circuit designs and we state the used measurement devices used to benchmark the developed amplifier. Finally, we give a step by step solution for creating a printed circuit board (PCB) containing our final design.

3.1 Measurement devices

To realize and benchmark the cryogenic amplifier, we used the following devices:

- CoppermountainTech. Planar 304/1 Vector Network Analyzer (VNA). The VNA was used to measure the Rf-output of the amplifier.
- Tektronix PWS2721 Power supply. This was used to bias the Hemt in saturation.
- Femto IV-converter. The Femto was used to measure the DC output of the amplifier.
- Tektronix TBS1052B oscilloscope.
- Unisoku USM1500 Scanning Tunnelling Microscope.
- RHK R9 STM controller.
- Warm amplifier: 2x Mini-circuit ZFL-1000LN+, + 2x (-3dB) attenuator (total gain $\approx$+44.6dB).

3.2 Single tank amplifier

3.2.1 General overview

Our initial design was the Single tank circuit. It was based on the ideas of Di Carlo et al. [6] and Arakawa et al. [7] and looked like this:

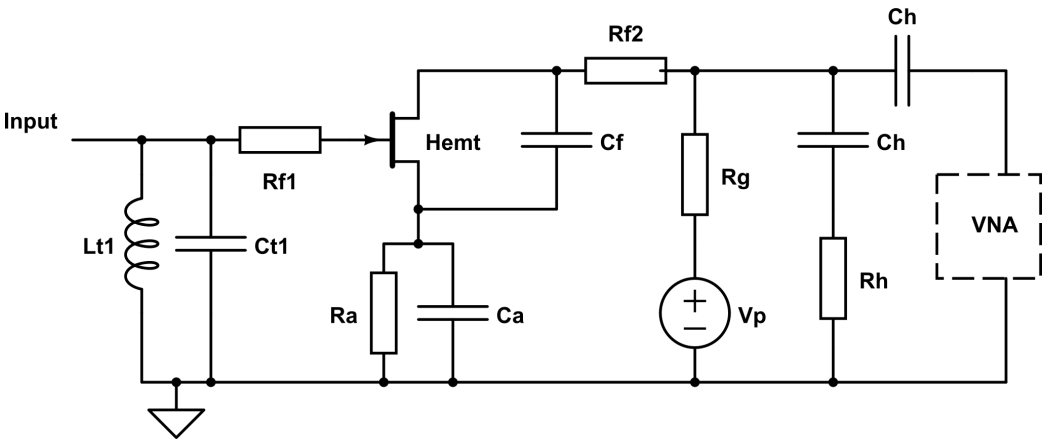

Figure 3.1: *Schematic drawing of the Single tank amplifier circuit. The 2 main components are the tank (L_t and C_t resonator), which translates the tunnelling current to a voltage on the gate of the Hemt (ATF-34143) and the Hemt itself, which acts as an amplifier and matches the impedance of our tunnel junction to the standard 50Ω of our measurement devices.*

The main idea behind this circuit is that the tunnelling current flows into a LC-resonator (L_t, 66μH, and C_t, 47pF), which translates this tunnelling current into a voltage on the gate of a saturated Hemt (ATF-34143). This voltage induces a current, which flows in an already matched 50Ω circuit, eliminating the need for further impedancematching.
V_p is there to bias the Hemt, together with R_g and R_a, which fix the bias point of the Hemt. R_g and R_a were chosen to be 1000Ω respectively 150Ω to bias the Hemt in saturation when V_p is set around 5V (see figure 3.2).

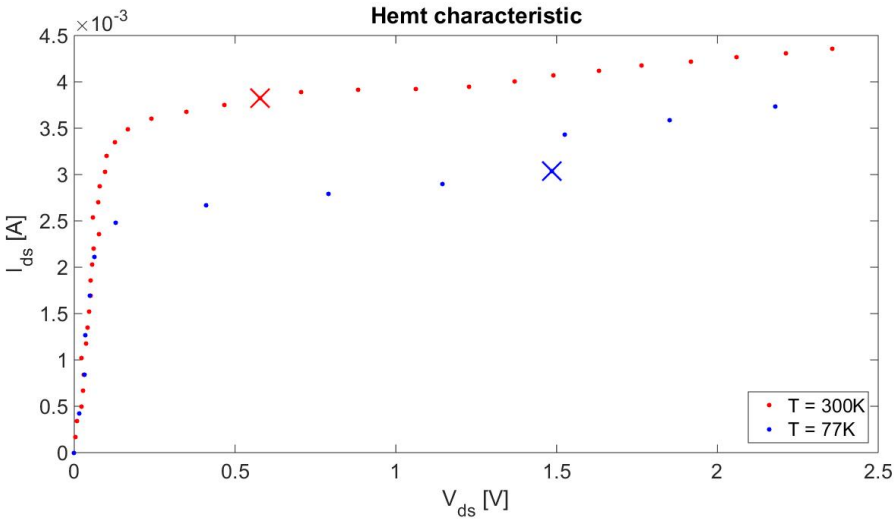

Figure 3.2: *Measurement data of a Hemt (ATF-34143) characteristic at 300K and 77K. The red and blue cross indicate the bias point when V_p = 5V.*

Capacitors C_h (22nF) are there to prevent DC current from flowing into the VNA and to retain the DC bias circuit for the Hemt. R_h was chosen to be 50Ω, in order to match the amplifier to our measurement electronics. Rf1 and Rf2 are 2 low ohmic (10Ω) resistors that terminate possible resonances from the tank with the Hemt, and C_f is a 10pF capacitor that provides extra stability for the Hemt. C_a (15nF) enhances transconductance of the Hemt at higher frequencies.
Because STM is built around reading the DC tunnelling current, and using that to control the distance between tip and sample (through a feedback mechanism), our amplifier also needs to have a DC output. The idea is that this DC current can be measured where L_t goes to ground: by connecting the standard STM feedback after the inductor in the tank, one could measure both the high frequency output (Rf output) with the VNA, and the DC current with the Femto IV converter. Sadly, this did not work out for us because of current leaking through the gate of the Hemt (see section 4.1.1: DC output) and hence, we had to redesign our amplifier, which gave us the Double tank circuit.

3.2.2 Simulations Rf output

Before testing our amplifier, we made a simulation of the Rf output in Matlab (see Appendix B).

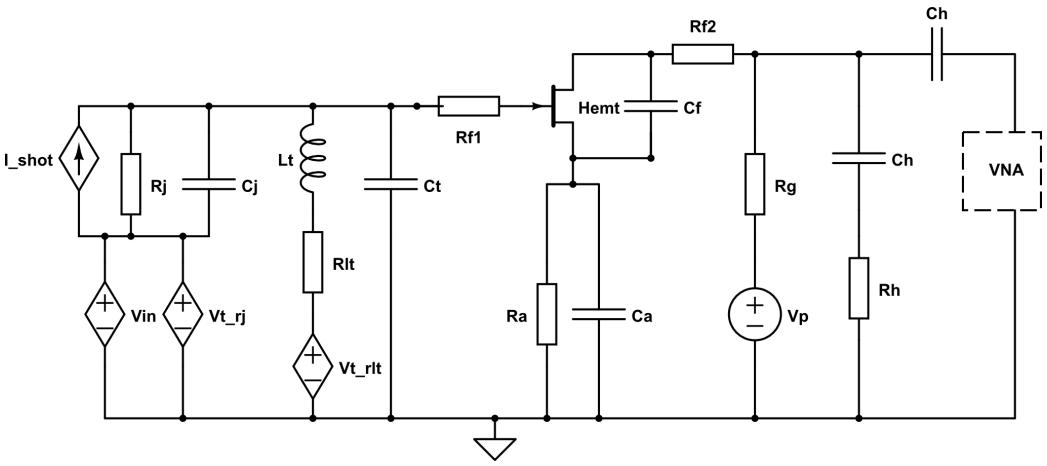

Figure 3.3: *Schematic drawing of the single tank amplifier circuit connected to a tunnel junction simulator (resistor R_j and capacitor C_j). Vt_{rj} and Vt_{rlt} are the thermal noise of the junctionsimulator (R_j) and the inductor (R_{lt}).*

Figure 3.3 shows a diagram of the circuit we simulated in Matlab, representing the single tank amplifier circuit. This figure also includes all the noisesources we took into account in our simulation, with the exception of the Hemt inputnoise (Voltagenoise, 0.4nV/sqrt(Hz)). We also added this to our simulation. The value is based on [6]
Note that we only took into account the sources in front of the Hemt, because these are the sources that get amplified by the Hemt. Furthermore, it includes R_{lt}, the total DC resistance of the inductor used in the tank. At room temperature (77K, 4K), R_{lt} = 26Ω (3.6Ω, 0.3Ω). We measured this with a conventional multimeter, except for the DC resistance at 4K, which we got from literature (We used the same inductors). [6].

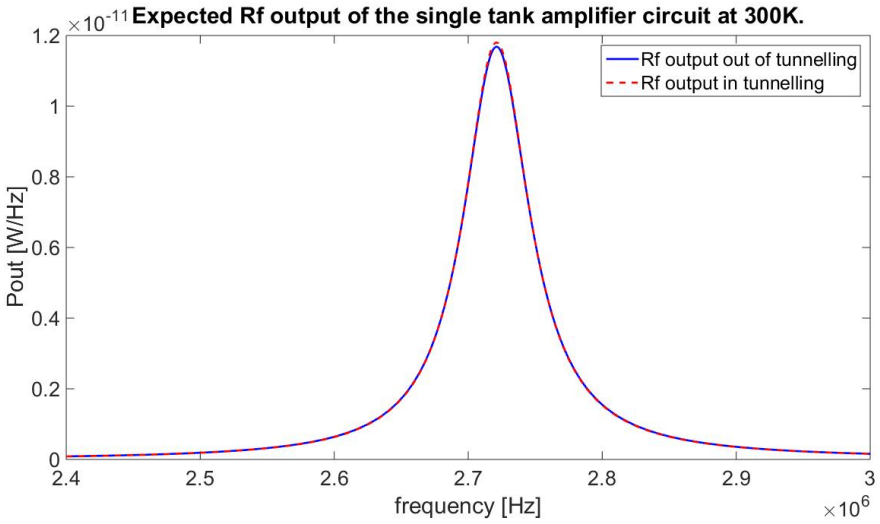

Figure 3.4: *Simulation of the output signal of the single tank amplifier (300K) due to thermal noise of the amplifier itself and shotnoise. The bias voltage (V_{in}) was set to 1V. The junction parameters are: $R_j = 50M\Omega$, $C_j = 70fF$. The simulation shows the power amplified by the warm amplifier. If we bring the tip in tunnelling, the signal we measure should increase by 1.03% due to the contribution of shotnoise.*

Figure 3.4 shows the result of our Matlab simulation for the Rf output of the single tank circuit. The dampening of the resonance peak is caused by the finite DC resistance of the inductors. This causes our overall amplification to be lower, which is devastating for measuring shotnoise (figure 3.4). Luckily, we can work around this by cooling our amplifier down (figure 3.5, 3.6). Figure 3.4, 3.5 and 3.6 show the contribution of shotnoise to the total signal at different temperatures. The simulated bias voltage was 1V and the junction parameters are $R_j = 100M\Omega$, $C_j = 30fF$.

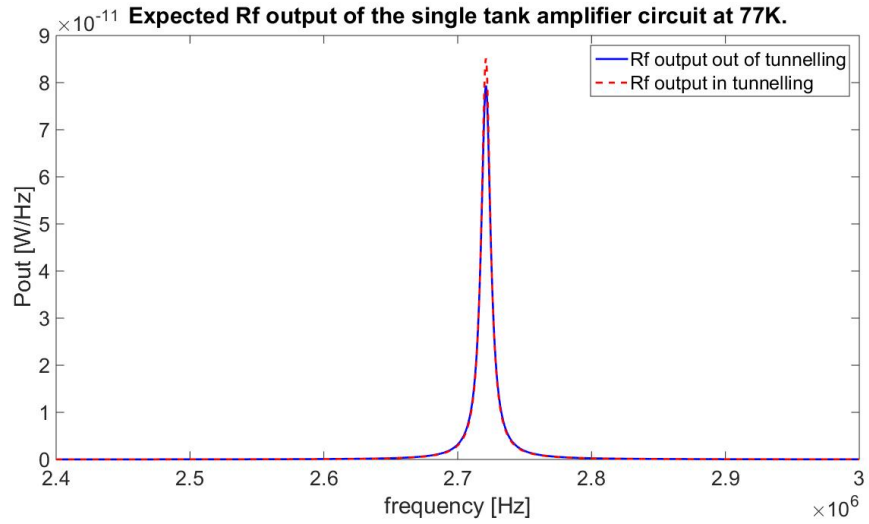

Figure 3.5: *Simulation of the output signal of the single tank amplifier (77K) due to thermal noise of the amplifier itself and shotnoise. The bias voltage (V_{in}) was set to 1V. The junction parameters are: R_j = 100MΩ, C_j = 30fF. The simulation shows the power amplified by the warm amplifier. If we bring the tip in tunnelling, the signal we measure should increase by 7.27% due to the contribution of schotnoise.*

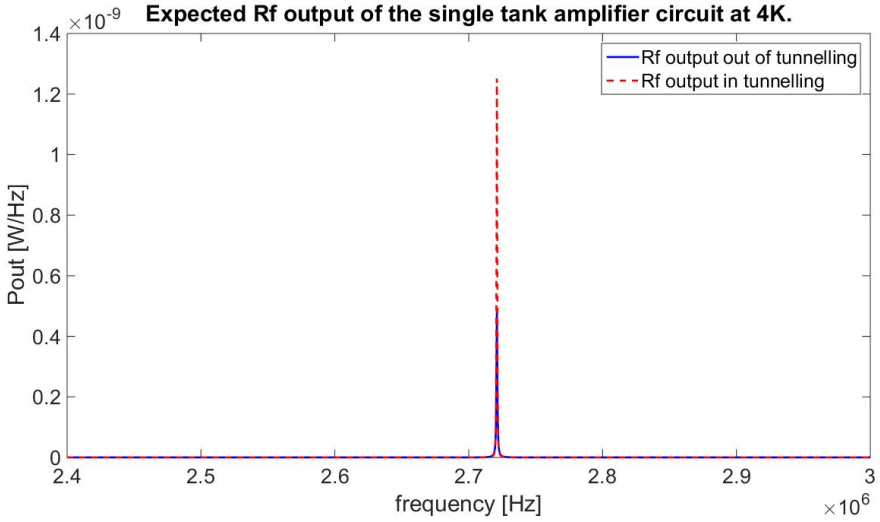

Figure 3.6: *Simulation of the output signal of the single tank amplifier (4K) due to thermal noise of the amplifier itself and shotnoise. The bias voltage (V_{in}) was set to 1V. The junction parameters are: R_j = 100MΩ, C_j = 30fF. The simulation shows the power amplified by the warm amplifier. If we bring the tip in tunnelling, the signal we measure should increase by 160% due to the contribution of schotnoise.*

Judging from figure 3.4, 3.5 and 3.6, we have no chance of measuring shotnoise at room temperature because the increase in signal is barely noticeable, however, at 77K and 4K, it should be possible. This is because as stated before, the DC resistance of the inductors decrease, increasing the Q factor of the tank, therefore increasing the amplification of our amplifier and therefore the magnitude of the total signal measured. Furthermore, decreasing temperature of course decreases the thermal noise of the amplifier itself, increasing the ratio of shotnoise to thermal noise of the signal.

3.3 Double tank amplifier

3.3.1 General overview

To stop the current leaking from the Hemt from mixing with the tunnelling current, we block it of with a capacitor. The problem with this solution is that the gate of the Hemt still needs to be connected to ground in order for it to function properly. Hence, we came up with the circuit in figure 3.7.

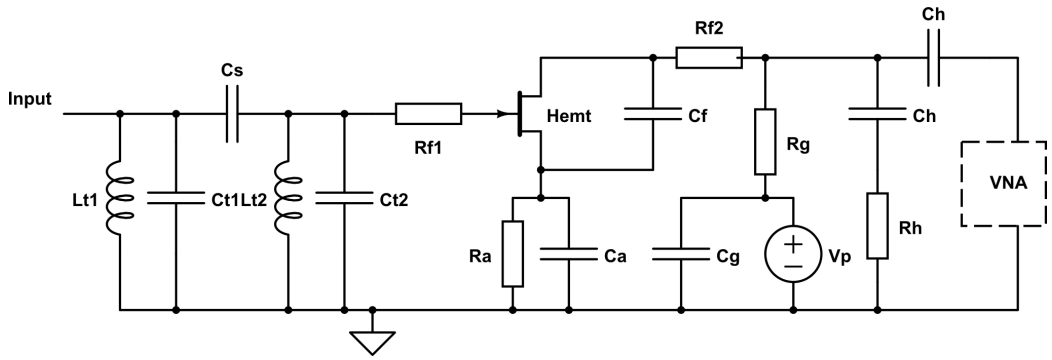

Figure 3.7: *Schematic drawing of the double tank amplifier circuit connected to a tunnel junction (resistor R_j and capacitor C_j). The main difference from the single tank circuit is as the name suggests: This circuit consists of 2 LC resonators. The first tank gives us a possibility to measure the DC tunnelling current, whereas the second tank function as a DC ground for the Hemt.*

As you can see from figure 3.7 and as the name of the circuit already suggests, the main difference between the double tank circuit and the original design is that instead of one LC resonator, we use two. The first tank (L_{t1} = 66μH, C_{t1} = 15pF) gives us a way to measure the DC tunnelling current for our STM feedback, whereas the second tank (L_{t2} = 66μH, C_{t2} = 15pF) provides a DC ground for the gate of the Hemt. The value for C_{t1} is chosen different from C_{t2} on purpose, in order to compensate for the capacitance

of the cable coming from the tip to the amplifier (in our setup, $\pm$30pF). To block the DC leakage from the Hemt, C_s (22nF) was installed to connect the two tanks. Intuitively, one could say that this capacitor should be as big as possible so that Rf signal could pass easily, and in principle this is true. The two tanks could then be seen as one single tank with $L_{total} = \frac{Lt}{2}$ and $C_{total} = 2 * Ct$, making the entire structure resonate at the same frequency as the single tank circuit. However, the problem here lies with the DC output. When we say that the STM feedback relies on measuring the DC tunnelling current, this is true, but it also needs a few higher frequencies because otherwise the feedback becomes too slow. To calculate the optimal value for C_s, we simulated the DC output for different frequencies in Matlab (figure 3.8). As you can see, if we choose the capacitor to be of the order of tens of microfarats, the DC-output has a cut-off and the feedback is too slow. However, if we decrease the capacitance, we see that the bandwidth goes asymptotically to a certain optimum.

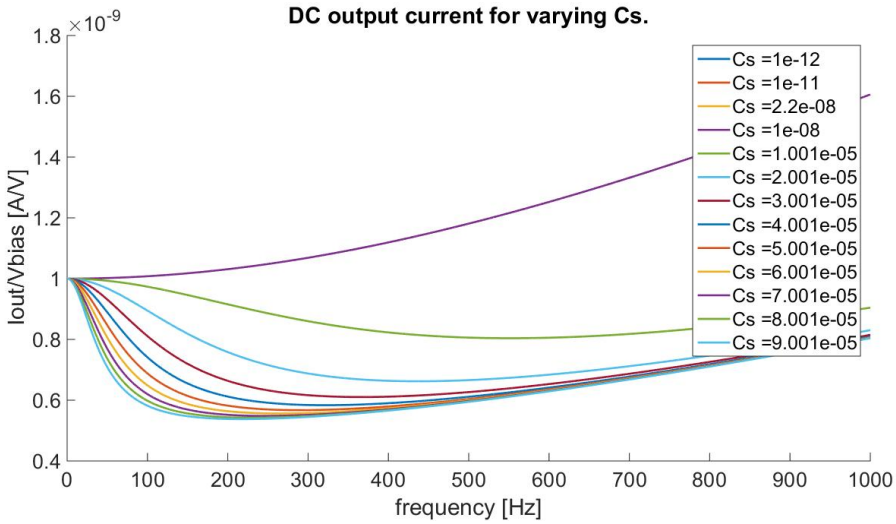

Figure 3.8: *Simulation of the DC output current divided by applied bias voltage, as function of frequency. Notice that the bandwidth stays constant for $C_s \leq$ 1nF, but decreases if $C_s >$ 1nF.*

Finally, another change we made with respect to the single tank circuit was that we added C_g (22 μF). This capacitor is there to make sure R_g is connected to ground, because even though in theory a voltage supply has zero resistance, we put the extra capacitor there to make sure this was not a topic to be concerned about. Furthermore, it filters out any high frequency noise coming from the voltage source.

3.3.2 Simulations Rf output

Similar to what we did with the single tank circuit, before building the double tank amplifier, we simulated the Rf output in Matlab. Figure 3.9 shows an overview of the circuit we simulated.

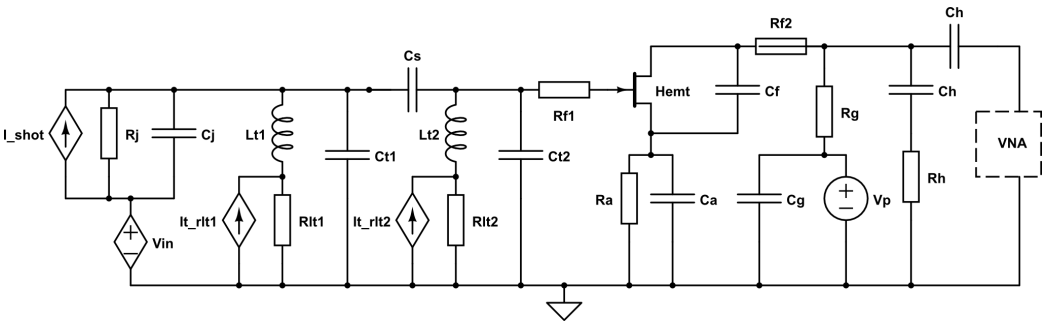

Figure 3.9: *Schematic drawing of the double tank amplifier circuit connected to a tunnel junction simulator (resistor R_j and capacitor C_j). Vt_{rj}, Vt_{rlt1} and Vt_{rlt2} are the thermal noise of the junctionsimulator (R_j), the inductor in the first tank (R_{lt1}) and the inductor in the second tank (R_{lt2}) respectively.*

As you can see from figure 3.10, the double tank circuit has the same problem as the single tank circuit, in the sense that it won't work at 300K due to the DC resistance of the inductors. However, judging from figure 3.11 and 3.12, the double tank circuit can work at 77K and especially at 4K.

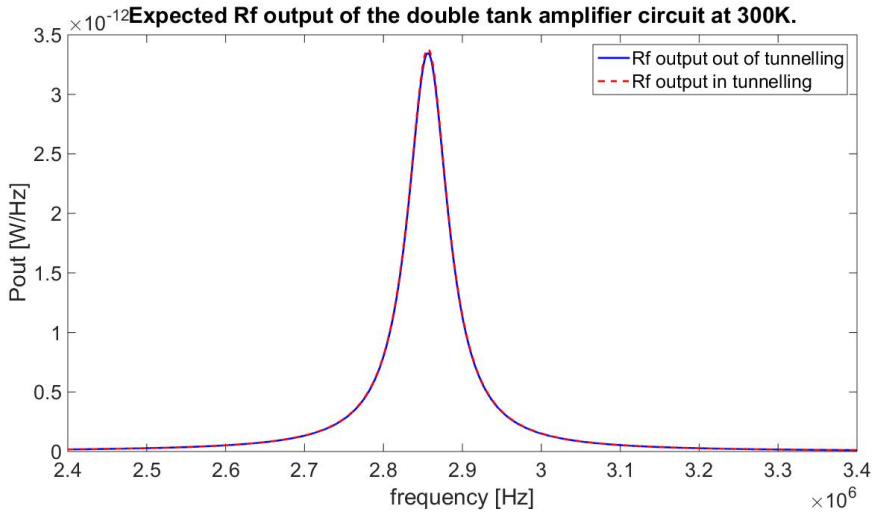

Figure 3.10: *Simulation of the output signal of the double tank amplifier (300K) due to thermal noise of the amplifier itself and shotnoise. The bias voltage (V_{in}) was set to 1V. The junction parameters are: R_j = 50MΩ, C_j = 70fF. The simulation shows the power amplified by the warm amplifier. If we bring the tip in tunnelling, the signal we measure should increase by 1.04% due to the contribution of shotnoise.*

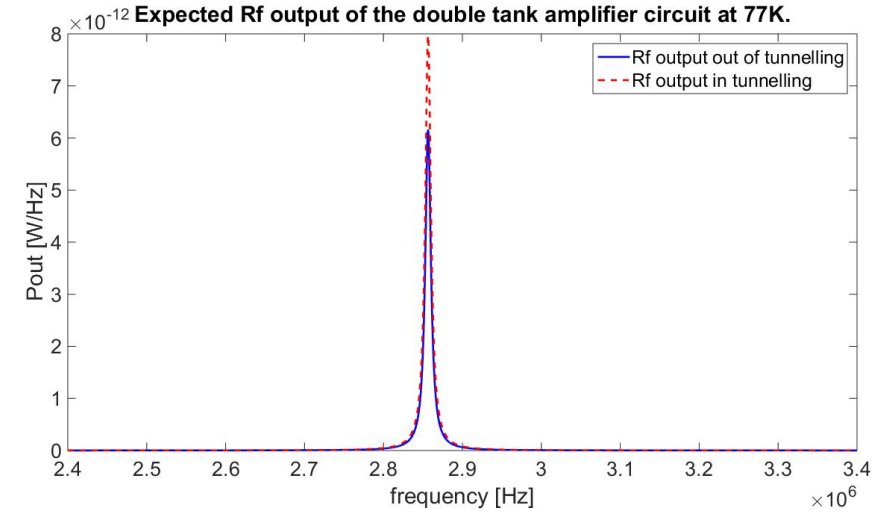

Figure 3.11: *Simulation of the output signal of the double tank amplifier (77K) due to thermal noise of the amplifier itself and shotnoise. The bias voltage (V_{in}) was set to 1V. The junction parameters are: R_j = 50MΩ, C_j = 70fF. The simulation shows the power amplified by the warm amplifier. If we bring the tip in tunnelling, the signal we measure should increase by 29.4% due to the contribution of shotnoise.*

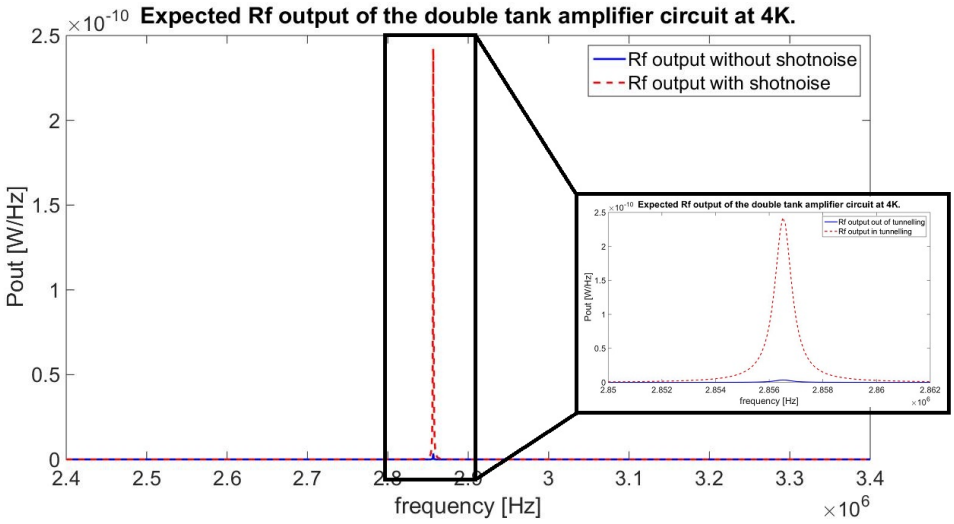

Figure 3.12: *Simulation of the output signal of the double tank amplifier (4K) due to thermal noise of the amplifier itself and shotnoise. The bias voltage (V_{in}) was set to 1V. The junction parameters are: $R_j = 50M\Omega$, $C_j = 70fF$. The simulation shows the power amplified by the warm amplifier. If we bring the tip in tunnelling, the signal we measure should increase by 6779% due to the contribution of shotnoise.*

3.4 Alternative circuit

As an alternative to our double tank amplifier circuit, we would like to present another possible solution (figure 3.13).

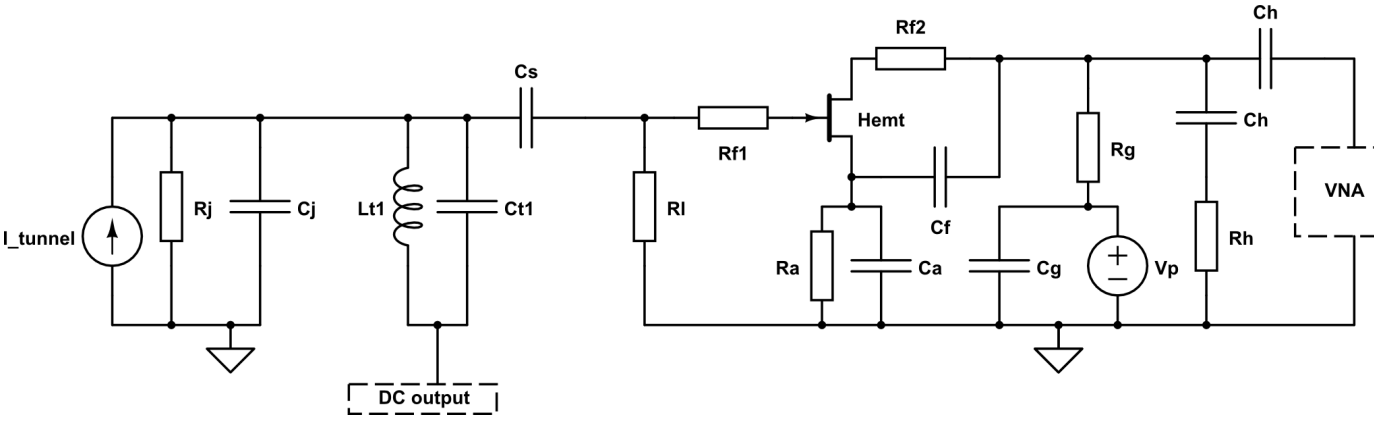

Figure 3.13: *An alternative circuit for the cryogenic amplifier. Instead of having a second tank, a big resistor is placed in front of the Hemt to translate the tunnelling current into a gate voltage.*

Instead of having a second tank, a big resistor is placed in front of the Hemt to translate the tunnelling current into a voltage on the gate of the Hemt. The leakage current from the Hemt would still be blocked and is grounded through this resistor. We tried to make this work with R_l = 50MΩ, but unfortunately this circuit did not give any Rf response, i.e, the Hemt was saturated, but upon checking the Rf output of the amplifier, it would just give us a flat signal. There can be multiple explanations for this, but one of them is for example that the smd resistor, even though we thought it to be high impedant, it might not have been for Rf signals since resistors always carry a certain parasitic capacitance with them.
We did not investigate this problem further since we saw two clear downsides with this solution:

1. An extra noise source is introduced in the amplifier.
2. We want the impedance that translates the tunnelling current to a voltage to be big (bigger impedance equals bigger voltage). Since a resonator in theory can reach infinite impedance, there are no resistors that can compete with this.

3.5 PCB making

In this section, we describe the materials needed to make our cryogenic amplifier. Furthermore, we give a step by step guide and present our result.

3.5.1 Materials needed

- TMM10i Printed circuit board material (42x20mm for 1 amplifier).
- Kontakt Chemie photo sensitive lacquer (20) (Film resist).
- Thick transparent tracing paper.
- 0.1M NaOH solution.
- $FeCl_3$ etchant ($\sim$ 250g/l).
- Acetone.

Also, a laser printer and a UV lightsource are required.

3.5.2 Guide

1. Print the mirrored PCB layout (Appendix A) on the tracing paper with a laser printer.

2. Coat the PCB material with film resist and let it dry for 24 hours in a dark place. Optionally, you could also bake it in an oven ($\pm$15min, 70°C).

3. After the Resist has dried, cut out the PCB layout from the tracing paper and put it on the PCB material, in such a way that the toner makes contact with the copper. Secure it in place with scotchtape or other see through tape. This will function as a mask for the filmresist.

4. Light the PCB with UV light. Depending on the intensity of the light, light it for approximately 1 to 3 minutes. After that, take of the mask.

5. Develop the PCB in 0.1M NaOH solution (approximately 5 minutes).

6. Etch the PCB with a $FeCl_3$ solution. The concentration and temperature of the solution can be varied to speed up the etching process, but we used 250g/l $FeCl_3$ at room temperature. It took us approximately 15 minutes.

7. After all excess copper has been removed from the PCB, rinse it under a sink. This is to make sure all the $FeCl_3$ is washed off in order to stop the etching process.

8. Clean the PCB with acetone to remove the remaining resist.

3.5.3 Result

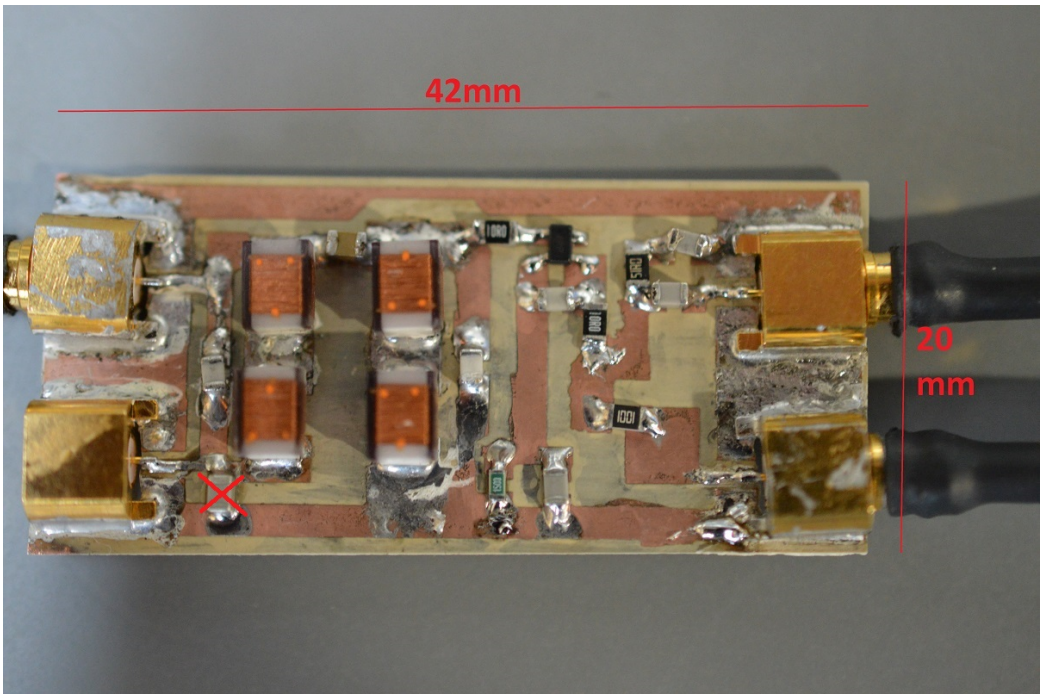

Figure 3.14: *Picture of the home made PCB containing the double tank amplifier circuit. This is the PCB that is implemented in our STM setup. The crossed out capacitor is a component we took out in our final design and which is also not shown on the circuit drawings.*
The dimensions of our PCB are 42mm x 20mm.

Chapter 4

Building and testing the cryogenic amplifier

4.1 Amplifier test results

To tune and test our amplifier, we performed the following tests:

- Calibrate the Hemt bias: for each circuit containing a Hemt, we measured I_{ds} as function of applied voltage between source and drain, V_{ds}. During this measurement, the Hemt gate is connect to ground. This curve allows us to find an optimal value for the Hemt bias, making sure it is in the saturated regime.
  I_{ds} is measured with a conventional multimeter capable of measuring in μA range. V_{ds} is varied by manipulating the Hemt bias: Say we set the Hemt bias to xV, then $V_{ds} = x - I_{ds} * (150 + 1000)$ (150 and 1000 are the values of the resistors in series with the Hemt source- and draincontacts, see figure 3.2.

- Measure the Rf output of the amplifier, giving Rf input: We measure the Rf response of our amplifier when we manually put a white power spectrum in with the VNA. This allows us to extract the transfer function of our amplifier. For this test, a 100MΩ (50MΩ) smd resistor was put in front of the (first) tank (in series with the input cable) in the single- respectively double tank circuit, to simulate a tunnel junction (Appendix C: figure C.1, C.2). The Rf output of the amplifier is connected to the warm amplifier, which in turn is connected to the VNA. All test measurements were performed in this setup. This test was done at room temperature, as well as at 77K

using a dipstick to submerge the electronics in a dewar of liquid nitrogen.

- Measure the Rf output of the amplifier, without input: In this test, the only sources are the thermal noise of the inductors and resistors in the amplifier. This is important should the amplifier be used to measure the absolute value of small signals in the future ($\leq pW/Hz$). Note that for a shot noise curve, this is less important since we are only interested in the relative change in height of the output power at a certain frequency, as function of bias voltage over the junction. This test was done both at room temperature and at 77K.

4.1.1 Single tank amplifier test results

Even though the single tank circuit is not our final design, the single tank circuit still proved quite useful for understanding the behaviour of the amplifier we were building. This is, because even though (as later described) the DC output of this amplifier does not work correctly, the Rf output is very similar to that of the double tank. Hence, understanding this circuit means that we have adequate knowledge about the individual components of the amplifier, and makes benchmarking of the double tank circuit just a matter of verification.

Rf output at room temperature

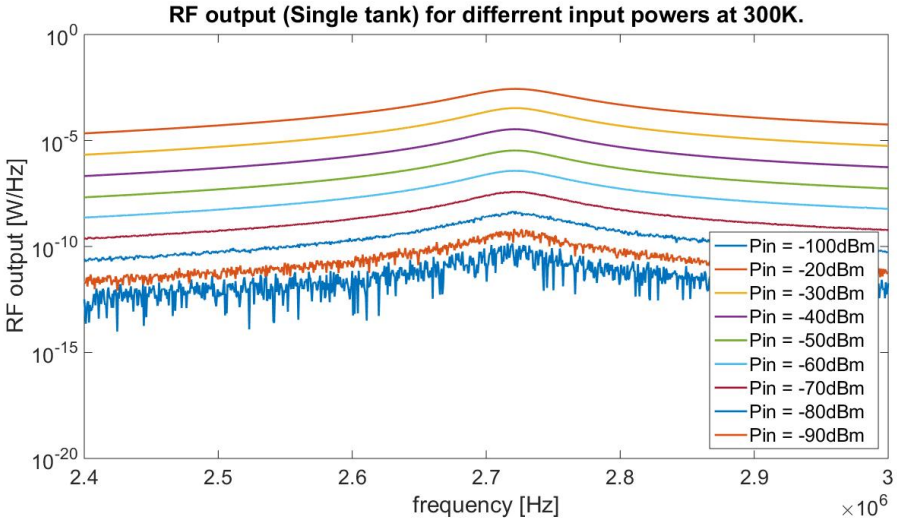

Figure 4.1: *Rf-output of the single tank circuit for different input powers (Measured at room temperature). The data was measured with an IF bandwidth of 100Hz and averaging 10 times (with the VNA).*

Figure 4.1 shows the measured Rf output of the amplifier for different input powers at room temperature. The Hemt bias supply was set to 4V. As you can see from the data, our amplifier resonates at roughly 2.72MHz.
The data from figure 4.2 was obtained in a similar way, except that now, there was no input power given. The 100MΩ smd resistor is still on the board, but since the noise is dominated by the inductors, we can neglect that. Therefore, this figure shows the noise characteristic of the amplifier itself.

Rf output at 77K

Figure 4.3 shows the Rf output of the amplifier for different input powers at 77K. As you can see, when the amplifier is cooled down, the peak gets a bit sharper and shifts from 2.72MHz to 2.76MHz with respect to the results at room temperature. This can be explained by the capacitor in the tank: It is very plausible that at 77K, its impedance is higher because the capacitor shrinks a bit.
Figure 4.4 shows the noise characteristic of the amplifier at 77K. If we compare this to figure 4.2, we see that the maximum noise power has decreased. This is of course because all of the noisesources in our amplifier

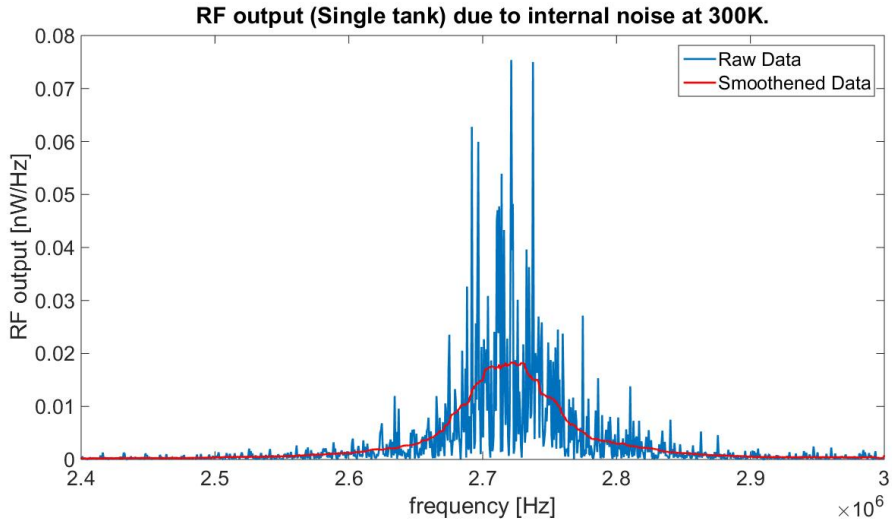

Figure 4.2: *Rf-output of the single tank circuit without input (Measured at room temperature). The blue line is the data collected by the VNA, whereas the red line is a moving average of the blue line. The data was measured with an IF bandwidth of 100Hz and averaging 10 times (with the VNA).*

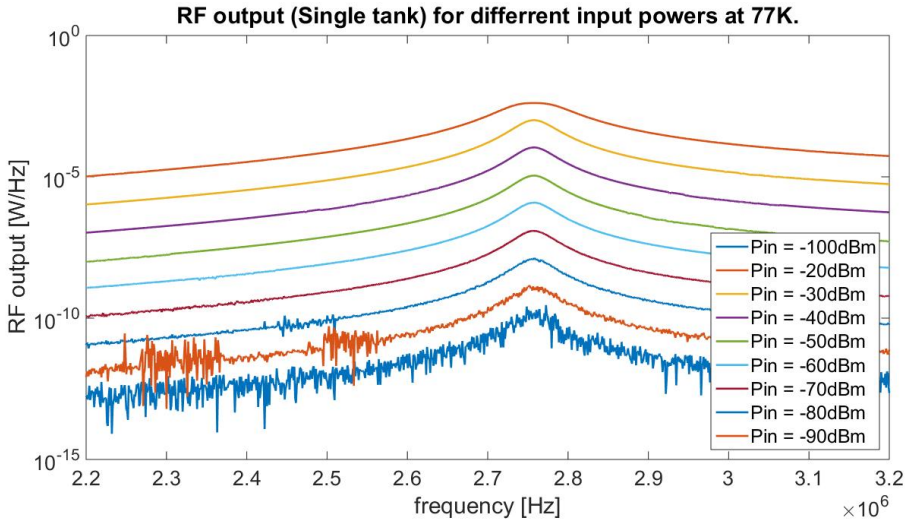

Figure 4.3: *Rf-output of the single tank circuit for different input powers (Measured at 77K). The data was measured with an IF bandwidth of 100Hz and averaging 10 times (with the VNA). Notice that the data collected for Pin = -20dBm seems to have a smaller Q factor. This exact reason for this is unclear to us, but it might be due to the fact that the amplifier wasn't fully cooled down yet, because Pin = -20dBm was the first measurement we did in this series.*

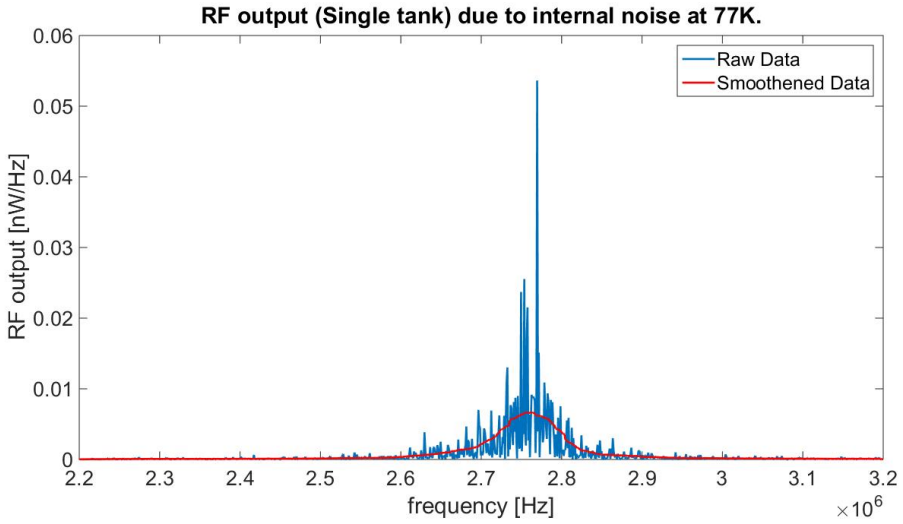

Figure 4.4: *Rf-output of the single tank circuit without input (Measured at 77K). The blue line is the data collected by the VNA, whereas the red line is a moving average of the blue line. The data was measured with an IF bandwidth of 100Hz and averaging 10 times (with the VNA).*

are of thermal origins and since we cool the amplifier down, we expect to measure less signal.

DC- output

To test the DC output of our amplifier, we put a DC voltage (0.1V) on the input of our amplifier. At the same time, we turn on the Hemt bias, since this mimics normal operating conditions for our amplifier. The DC output of the amplifier is connected to the Femto IV converter, which in turn is connected to an oscilloscope.
If we give 0.1V input, since there is a 100MΩ resistor in front of the cryoamp (to mimic a tunnel junction), we expected to measure roughly 1nA from the DC output. To our surprise however, we measured about 2nA. When we turned of the Hemt bias, the offset was gone and we measured the expected 1nA. This made us grow suspicious of the Hemt, and indeed, because of the finite gate- to source resistance of the Hemt, a current leaked through the Hemtgate. To solve this problem, we designed the double tank circuit: A capacitor blocks the current flowing through the Hemt gate from reaching the first tank. Instead, it flows away to ground via the second tank. The DC signal for the STM feedback is measured from the first tank (see figure 3.7).

4.1.2 Double tank amplifier test results

Rf output at Room temperature

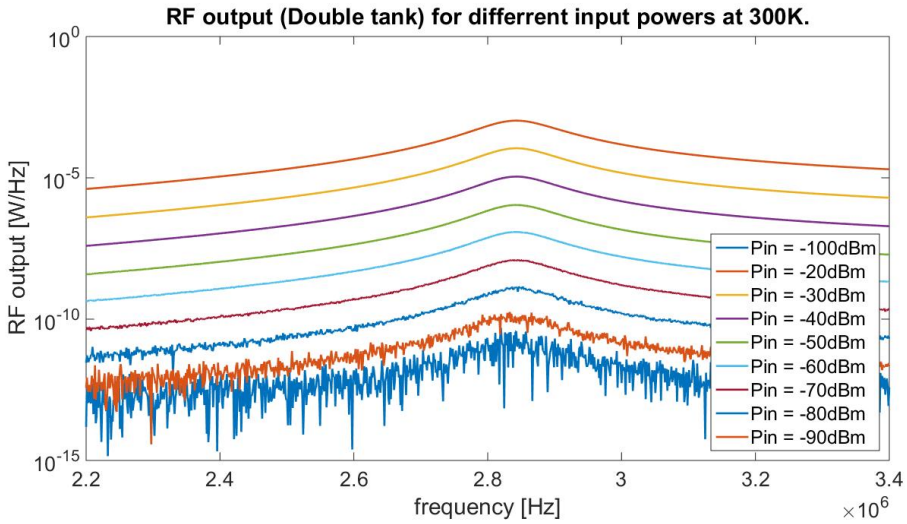

Figure 4.5: *Rf-output of the double tank circuit for different input powers (Measured at 300K). The data was measured with an IF bandwidth of 100Hz and averaging 10 times (with the VNA).*

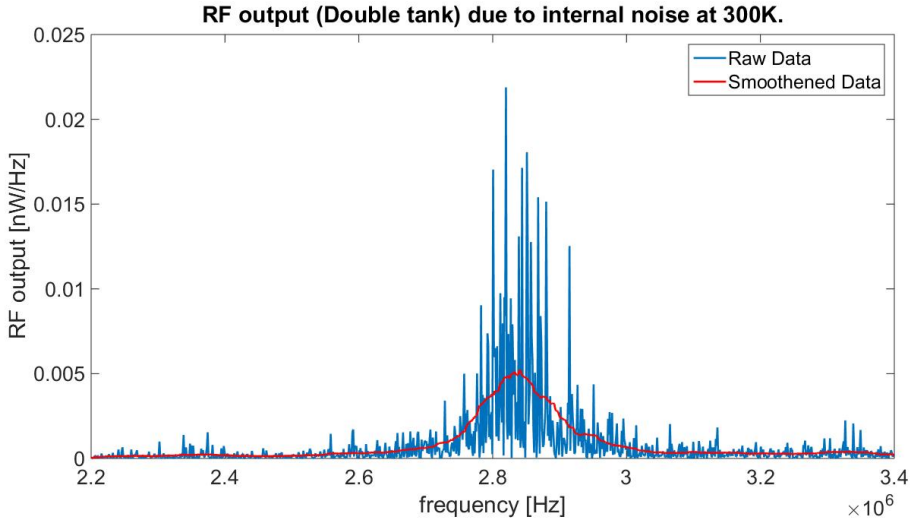

Figure 4.6: *Rf-output of the double tank circuit without input (Measured at 300K). The blue line is the data collected by the VNA, whereas the red line is a moving average of the blue line. The data was measured with an IF bandwidth of 100Hz and averaging 10 times (with the VNA).*

Rf output at 77K

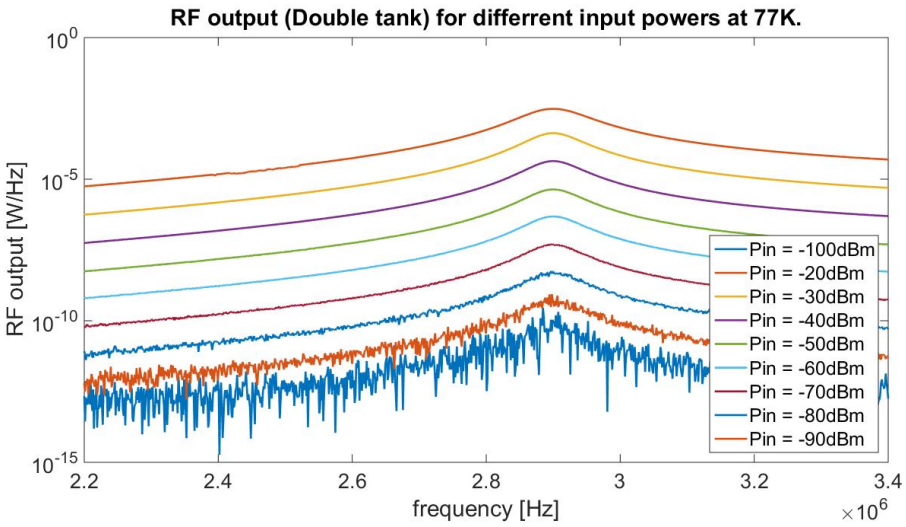

Figure 4.7: *Rf-output of the double tank circuit without input (Measured at 77K). The blue line is the data collected by the VNA, whereas the red line is a moving average of the blue line. The data was measured with an IF bandwidth of 100Hz and averaging 10 times (with the VNA).*

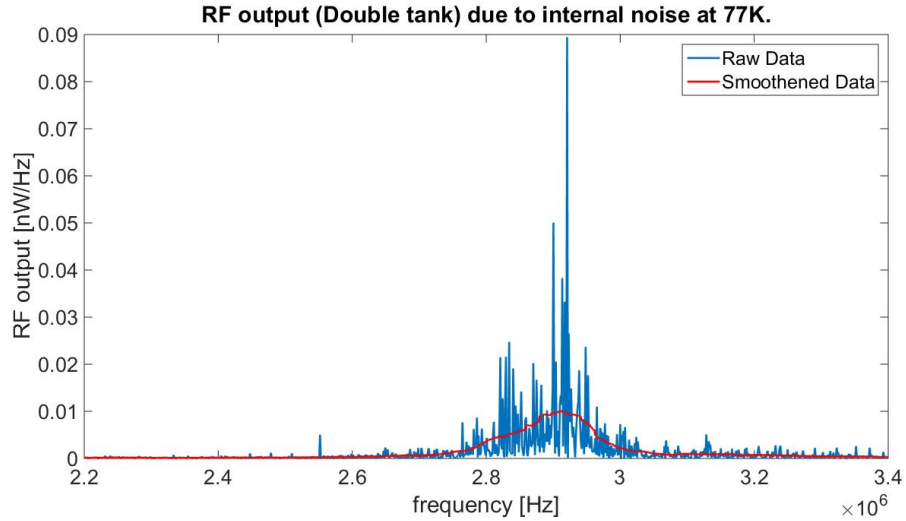

Figure 4.8: *Rf-output of the double tank circuit without input (Measured at 77K). The blue line is the data collected by the VNA, whereas the red line is a moving average of the blue line. The data was measured with an IF bandwidth of 100Hz and averaging 10 times (with the VNA).*

4.2 Amplifier test results from a STM setup

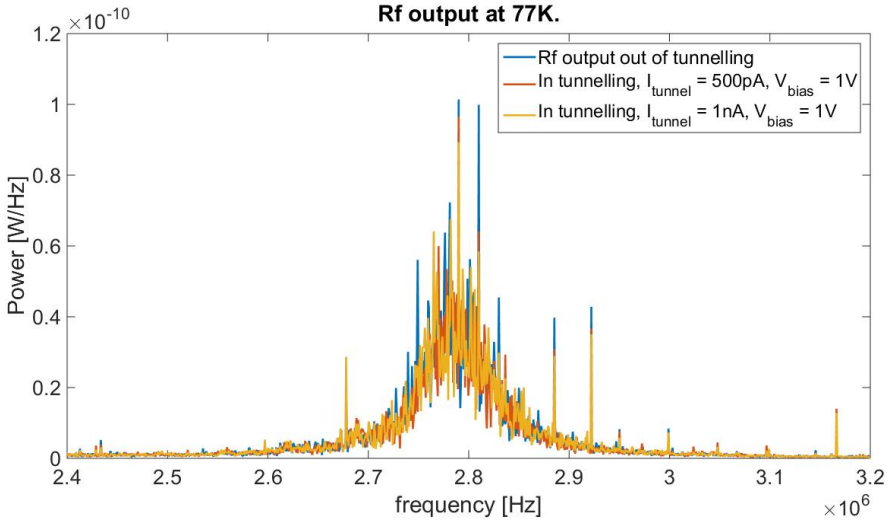

Figure 4.9: *Rf-output measured at 77K from a double tank amplifier implemented in our STM setup. The data was measured with an IF bandwith of 100Hz and later averaged in Matlab (10 measured spectra per measurement).*

We implemented our amplifier in a commercial STM setup (Unisoku USM1500) (figure 4.10, 4.11). We tried to measure shotnoise at 77K on a HOPG sample. Unfortunately, it seems that we have not yet been able to measure it because the gain of our amplifier in its current state is not large enough to be able to distinguish shotnoise from the thermal noise of the amplifier itself (figure 4.9).

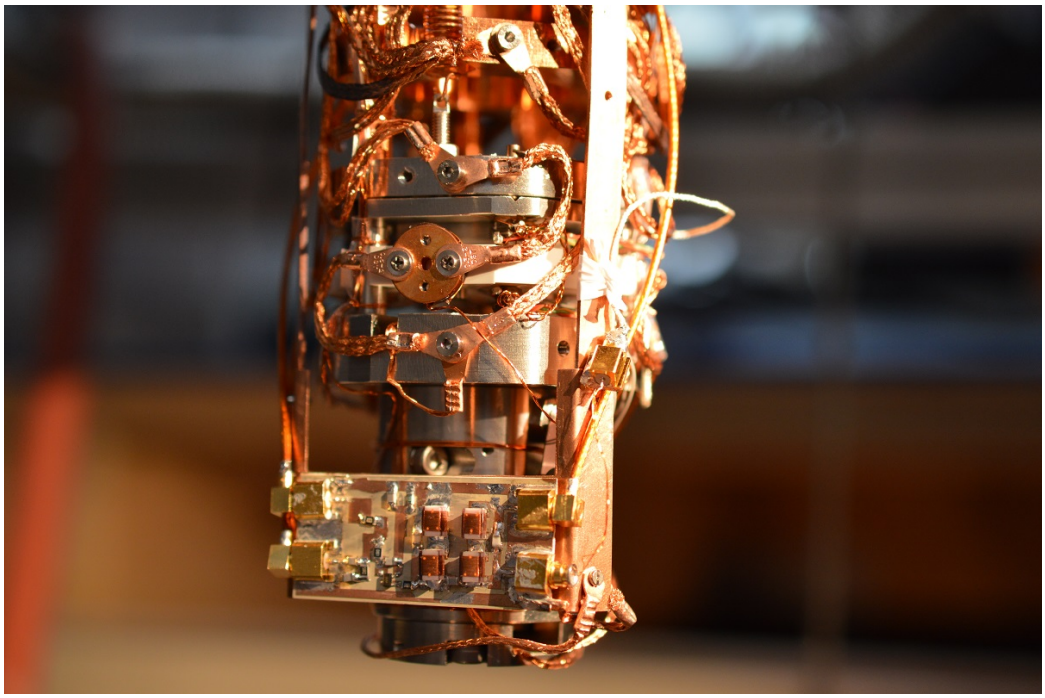

Figure 4.10: *Picture of the double tank amplifier installed in our Unisoku USM1500 STM setup. A custom mount was made out of copper, in order to attach the PCB to the STM frame. The PCB is glued to this mount with silver epoxy.*

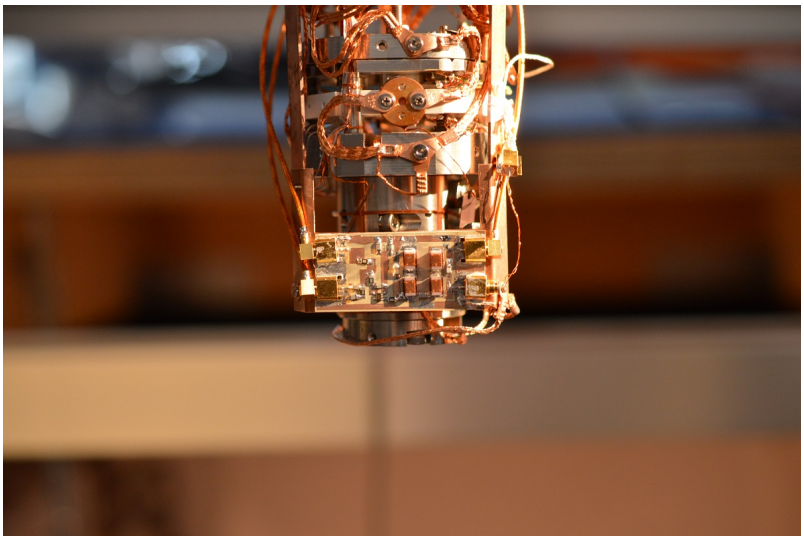

Figure 4.11: *Picture of the double tank amplifier installed in our Unisoku USM1500 STM setup. A custom mount was made out of copper, in order to attach the PCB to the STM frame. The PCB is glued to this mount with silver epoxy.*

4.3 Discussion

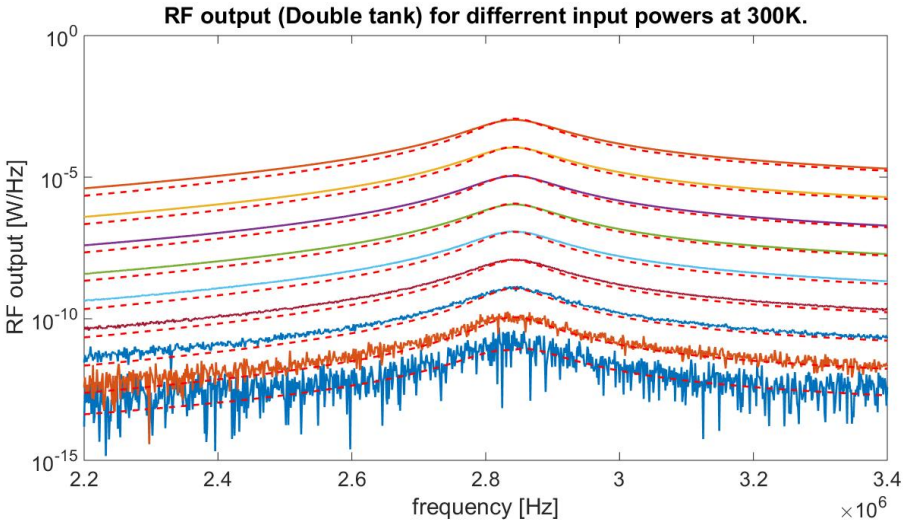

Figure 4.12: *Rf-output of the double tank circuit for different input powers (Measured at 300K), plotted against the simulated Rf-output. C_j = 42fF, R_{lt} = 40Ω.*

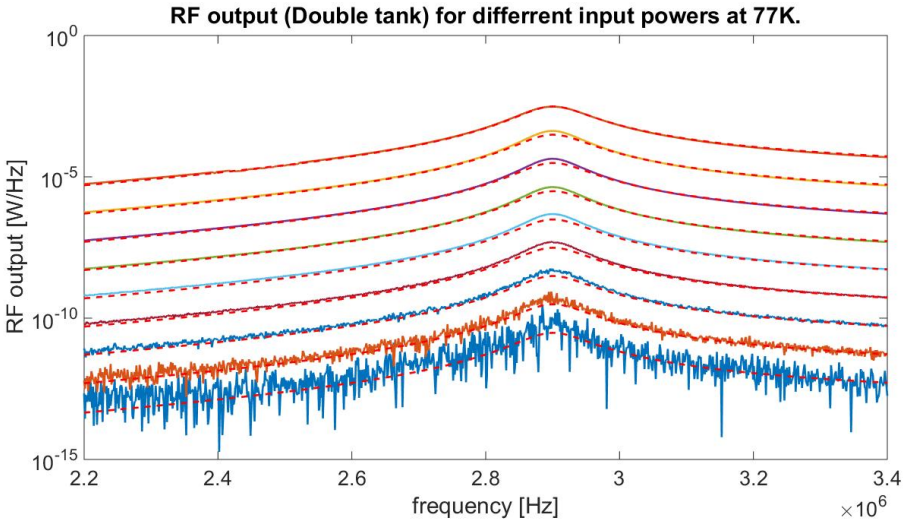

Figure 4.13: *Rf-output of the double tank circuit for different input powers (Measured at 77K), plotted against the simulated Rf-output. Cj = 78fF, Rlt = 40Ω.*

In this section, we would like to go over our test results again and compare them with simulations from the method section. We start of with the double tank amplifier circuit, since this is in the end our final design. Our

fitting parameters were the parasitic capacitance of the high ohmic junction simulator (R_j) (section 4.1) and the DC resistance of the inductors in both tanks (R_{lt}). We took this as a single fitting parameters since in both tanks, inductors of the same type were used.

Figure 4.12 shows the data from figure 4.5 with our simulation plotted through it. What's a bit curious is the fact that the fit value for the DC resistance of the inductors is 40Ω. Since we measured this to be 26Ω with a multimeter, this is definitely fishy. To check if this is correct, we measured an inductor with an impedance analyser and found that the resistance of the inductors at 2.8Mhz (1kHz, practically DC) equals 38Ω (25.8Ω). This extra resistance probably comes forth from the skin- and proximity effect, which basically comes down to eddy currents causing dissipation, limiting the quality of our inductors.
This problem becomes even more clear if we cool our amplifier down (figure 4.13).

For DC, we measured the resistance of the inductors to be 3.6Ω at 77K. However, as can be seen from figure 4.13, the resistance at 77K is still 40Ω, indicating that the skin- and proximity effect really limit the quality of our resonator.
What's clear from both figure 4.12 and 4.13 is that around resonance, the simulations seem to be quite accurate, whereas especially for lower powers, away from resonance, the simulation seems to break down a bit. This can be explained however from the perspective of the eddy currents. In our simulation, we fit a fixed value for the resistance of the inductors, however in reality, the skin- and proximity effect are dependent on frequency, causing the resistance of our inductors to become a function of frequency as well. The value that results from our fit corresponds to the value for the DC resistance at resonance, because that's the interval in which our fitting algorithm does most of its job and so the simulation is most accurate around resonance, but becomes worse for different frequencies.

Chapter 5

Outlook

Our final design for the amplifier is the double tank circuit. The main challenge we face now is that this design does not function as good as was expected from previous simulations because of the quality of the inductors we used in the tanks. To overcome this, we can think about replacing all inductor with superconducting coils. In this way, we would in theory not be bothered by the skin- and proximity effect. The downside of this solution is that the amplifier probably only works at 4K, depending on which superconducting material we use.
After implementing this, we believe there is a very real chance of measuring shotnoise with this amplifier. Once that has been achieved, we can think about programming the VNA to automatize shotnoise measurements: Measuring shotnoise curves simultaneous with making topographs of a sample.

Chapter 6

Acknowledgements

Since I am not sure how to phrase this, I am just going to say it like this:
I am really grateful to all of the people be it for interesting discussions, teachings, technical support or even moral support:

Members of the Allan lab:	**Others:**
Milan Allan	Kier Heeck
Koen Bastiaans	Bert Krama
Irene Battisti	Co Konings
Vitaly Fedoseev	Raymond Koehler
Maarten Leeuwenhoek	Peter van Veldhuizen
Oliver Ostojić	Freek Massee
Daniëlle van Klink	Nikolaos Iliopoulos
Arjo Andringa	
Gijsbert Verdoes	
Kees van Oosten	

Appendices

Appendix A

PCB layout

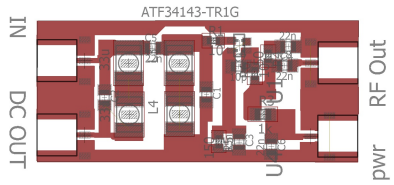

Figure A.1: *Layout of the PCB that was designed to hold our double tank circuit. For dimensions of the components, see table below.*

Component type	Dimension
SMP edgeconnector	figure A.2
Inductors	1812 imperial = 4532 metric
Resistors	0805 imperial = 2012 metric
Capacitors	0805 imperial = 2012 metric
Hemt (ATF-34143)	SOT-343

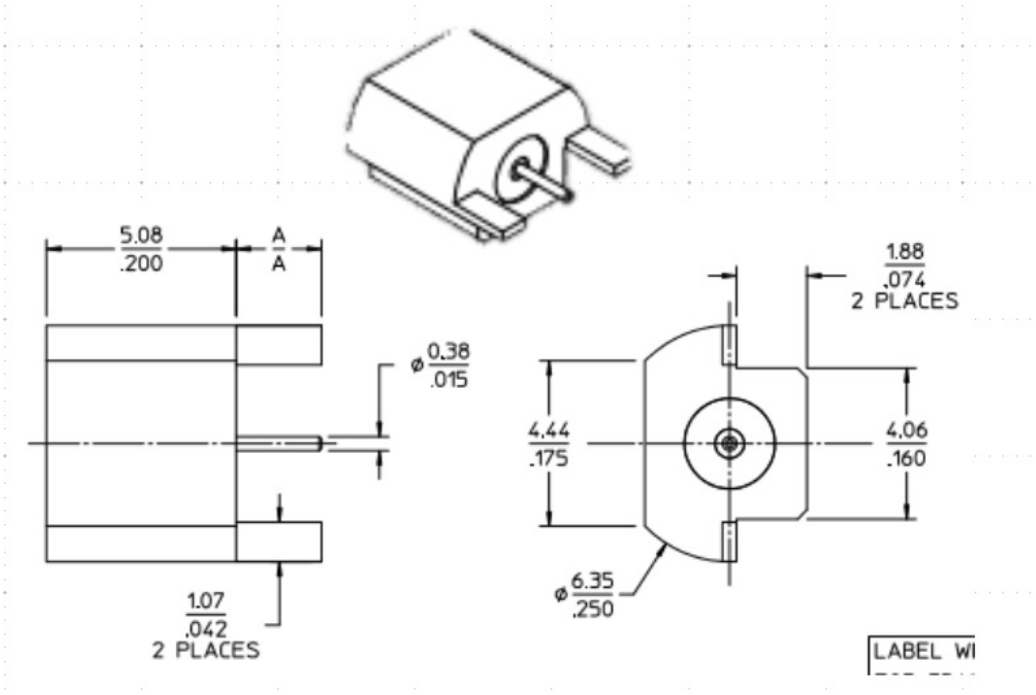

Figure A.2: *Overview of the dimensions of the SMP connector used on our PCB containing the double tank amplifier circuit.*

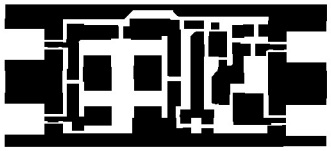

Figure A.3: *Mask of the PCB that was designed to hold our double tank circuit. This mask should be mirrored and printed on some tracing paper in order to use it for etching (section 3.5).*

Appendix B

Matlab code simulations

B.1 Single tank amplifier circuit simulation

```
function [Pout] = sim_singletank(f,T,Pin,fit)
%Simulation "just tank" circuit (= 1tank with attached 100Mohm)
    kb = 1.38064852e-23;

    gm = fit(3) * 1e-3; %transconductance Hemt

    Pin = 10^((Pin -30)/10);%dbm to Watt
    w = 2*pi*f;

    L_p = 66e-6;
    C_p = 51.8e-12;%capacitance tank + cable

    Rl_p = fit(2);

    Rvna = 50;
    Ccab = 100e-12;

    Rh = 50;
    Ch = 22e-9;
    Rg = 1e3;
    Ra = 150;
    Ca = 15e-9;

    Rj = 50e6;
    Cj = fit(1) * 1e-15;

    Zj = Zr([Z('R',Rj,w) Z('C',Cj,w)],'p',w);
    Zj = Zj*2;
```

```
29      Zt = Zr([Zr([Z('L',L_p,w) Z('R',Rl_p,w)],'s',w) ...
30          Z('C',C_p,w)],'p',w);
31
32      %thermal noise 100Mohm resistor
33      V_t_junction = sqrt(4*kb*T*Rj);
34
35      %thermal noise inductor
36      V_t_L = sqrt(4*kb*T*Rl_p);
37
38      Vin = sqrt(Pin*50);
39
40      H_prehemt = Zt ./ (Zt + Zj);
41
42      H_prehemt_inductornoise = Zr([Z('C',C_p,w) ...
43          Zr([Zj Zr([Z('R',Rvna,w) ...
44          Z('C',Ccab,w)],'p',w)],'s',w)],'p',w) ./ ...
45          (Zr([Z('C',C_p,w) Zr([Zj Zr([Z('R',Rvna,w) ...
46          Z('C',Ccab,w)],'p',w)],'s',w)],'p',w) ...
47          + Z('L',L_p,w) + Z('R',Rl_p,w));
48
49      V_hemtgate = sqrt((Vin * abs(H_prehemt)).^2 + ...
50          (V_t_junction * abs(H_prehemt)).^2 + ...
51          (V_t_L * abs(H_prehemt_inductornoise)).^2 +  ...
52          (0.4e-9).^2);
53
54      Za = Zr([Z('R',Ra,w) Z('C',Ca,w)],'p',w);
55
56      Id = gm*V_hemtgate .* (1./(1 + gm*Za));
57
58
59      Vout = abs((abs(Id) .* Z('R',Rh,w))./...
60       ( (Z('R',Rh,w) + Z('C',Ch,w))./Z('R',Rg,w) + 2));
61      G = gain_amp(f);
62      Vout = Vout .* sqrt(G);
63      Pout = Vout.^2 ./50;
64
65  end
```

B.2 Double tank amplifier circuit simulation

```
1  %Simulation double tank circuit (with inputpower possible)
2  function [Pout] = sim_doubletank(f,V_bias,T,Pin,fit)
3  %fit = [Cj Rlti_p gm]
4
5  %constants:
```

```
kb = 1.38064852e-23;
e = 1.60217662e-19;

w = 2*pi*f;

%Variables:
Rj = 50e6;
Cj = fit(1)*1e-15; %parasitic resistance of the high ohmic resistor.

Lt1_p = 67e-6;
Ct1_p = fit(4)*1e-12;

Cd_p = 100e-6;

Lt2_p = 67e-6;
Ct2_p = fit(5) * 1e-12;

Rlt1_p = fit(2);
Rlt2_p = fit(2);

Rg_p = 1e3;
Ra_p = 150;
Ca_p = 15e-9;

Rh_p = 50;
Ch_p = 22e-9;

gm = fit(3)*1e-3; %transconductance Hemt (A/V)

%Impedance shotcuts:
Zj = Zr([Z('R',Rj,w) Z('C',Cj,w)],'p',w);
Zt1 = Zr([Zr([Z('L',Lt1_p,w) Z('R',Rlt1_p,w)],'s',w) Z('C',Ct1_p,w)],'p',w);
Zt2 = Zr([Zr([Z('L',Lt2_p,w) Z('R',Rlt2_p,w)],'s',w) Z('C',Ct2_p,w)],'p',w);

Zd = Zr([Zr([Z('C',Cd_p,w) Zr([Zj Zt1],'p',w)],'s',w) Z('C',Ct2_p,w)],'p',w);
Za = Zr([Z('R',Ra_p,w) Z('C',Ca_p,w)],'p',w);

if V_bias == 0
    I_shotnoise = 0;
else
    I_shotnoise = sqrt(2 * e * (V_bias./Rj) * coth((e*V_bias)./(2*kb*T)));
end

I_t_1 = sqrt(4*kb*T/Rlt1_p) * ...
    ((1 + (Zt2 + Z('C',Cd_p,w)).*(1./Zt1 + 1./Zj))...
    ./(1 + (Zt2 + Z('C',Cd_p,w)).*(1./Z('C',Ct1_p,w) + 1./Zj))) .* ...
    (1./(1 + Z('L',Lt1_p,w)./Z('R',Rlt1_p,w) ...
    + (1./Z('R',Rlt1_p,w))./(1./Zj + 1./Z('C',Ct1_p,w) ...
    + 1./(Zt2 + Z('C',Cd_p,w))) ));
```

```
I_t_2 = sqrt(4*kb*T/Rlt2_p) * (Zd./Zt2) ...
    .* ( (1+(1./Zt1 + 1./Zj).*(Zt2 + Z('C',Cd_p,w)))...
    ./(1+(Z('L',Lt2_p,w) + Zd)./Z('R',Rlt2_p,w)) );
I_t_junction = sqrt(4*kb*T/Rj);

I_tot = sqrt(abs(I_shotnoise).^2 ...
    + abs(I_t_1).^2 + abs(I_t_2).^2 +...
    abs(I_t_junction).^2);
I_tot_o = sqrt(abs(I_t_1).^2 +...
    abs(I_t_2).^2 +  abs(I_t_junction).^2);

Pin = 10^((Pin - 30)/10);
Vin = sqrt(Pin * 50);

%Vg / Itot
H_tank = Zt2./( 1 + (1./Zj + 1./Zt1).*(Zt2 + Z('C',Cd_p,w)) );

Vg = sqrt((I_tot .* abs(H_tank)).^2 ...
    + (0.4e-9)^2 + ((Vin.*Zt2)./...
    (Zj + Zt2 + Z('C',Cd_p,w) + ...
    (Zj./Zt1) .*(Zt2 + Z('C',Cd_p,w)))).^2);
Vg_o = sqrt((I_tot_o .* abs(H_tank)).^2 ...
    + (0.4e-9)^2 + ((Vin.*Zt2)./(Zj + Zt2 ...
    + Z('C',Cd_p,w) + (Zj./Zt1) .*(Zt2 + Z('C',Cd_p,w)))).^2);

Id = abs((gm * Vg)./(1 + gm*Za));
Id_o = abs((gm * Vg_o)./(1 + gm*Za));

H_hemt = Z('R',Rh_p,w)./...
    (2 + (Z('R',Rh_p,w) + Z('C',Ch_p,w))...
    ./Z('R',Rg_p,w)); %(Vout/Id)

Vout = Id .* abs(H_hemt);
Vout_o = Id_o .* abs(H_hemt);

G = gain_amp(f);
Vout = Vout .* sqrt(G);
Vout_o = Vout_o .* sqrt(G);
Pout = Vout.^2/50;
Pout_o = Vout_o.^2/50;
end
```

B.3 Impedance calculation functions

```
function z = Z(t,m,w)
```

```
%function that returns an array
%with the complex impedance at
%specified frequencies.

if t == 'R' || t == 'r'
    z = ones(1,length(w)) * m;
elseif t == 'L' || t == 'l'
    z = 1i * w * m;
elseif t == 'C' || t == 'c'
    z = 1 ./ (1i * w * m);
else
    disp('Incorrect parameters');
end
```

```
function Zr = Zr(z,t,w)
%function returns the series or
%parallel impedance of 2 or more
%impedancearrays
    Zr = zeros(1,length(w));

    if strcmp('s',t) || t == 'S'
        for i = 1:1:length(w)
            for j = 0:length(w):(length(z)-length(w))
                Zr(i) = Zr(i) + z(i + j);
            end
        end
    elseif t == 'p' || t == 'P'
        for i = 1:1:length(w)
            for j = 0:length(w):(length(z)-length(w))
                Zr(i) = Zr(i) + (1 / z(i + j));
            end
        end
        Zr = 1./Zr;
    else
        disp('Incorrect input')
    end
end
```

Appendix C

Pictures of the test amplifiers

This appendix contains a picture of both the single tank amplifier test circuit and the double tank amplifier test circuit. These are different from the the real amplifier in the sense that they have a 100MΩ (50MΩ) smd resistor in front of the (first) tank (in series with the input cable) in the single- respectively double tank circuit, to simulate a tunnel junction (see figure C.1, C.2).

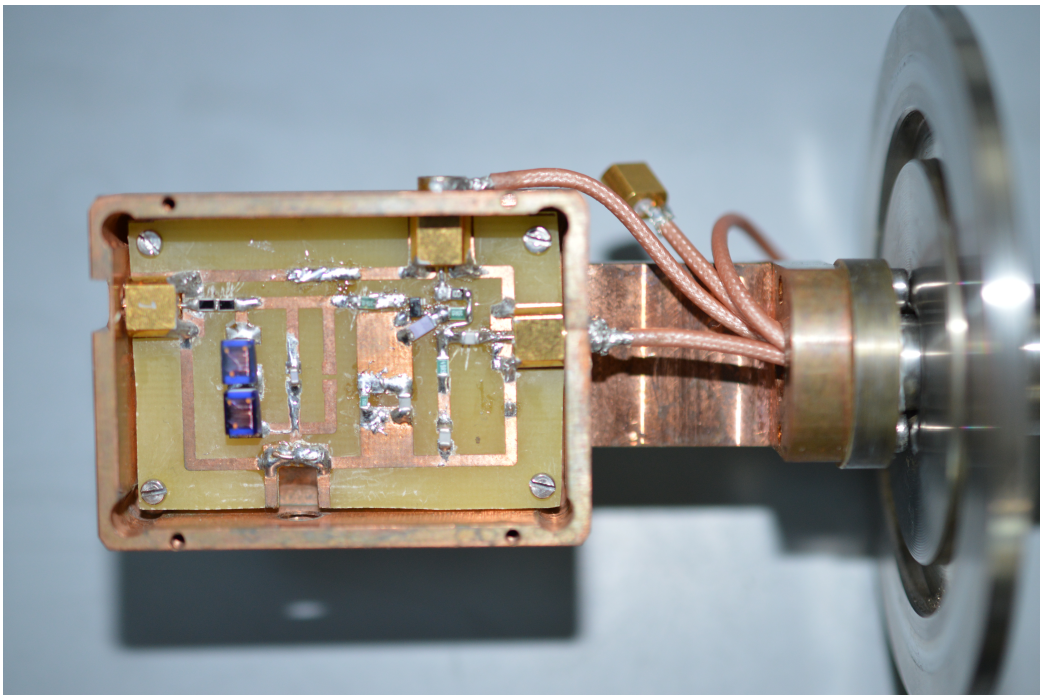

Figure C.1: *Picture of the single tank amplifier test circuit installed in our dipstick. Two 50MΩ smd resistors we're soldered in series in front of the tank, to simulate a tunnel junction.*

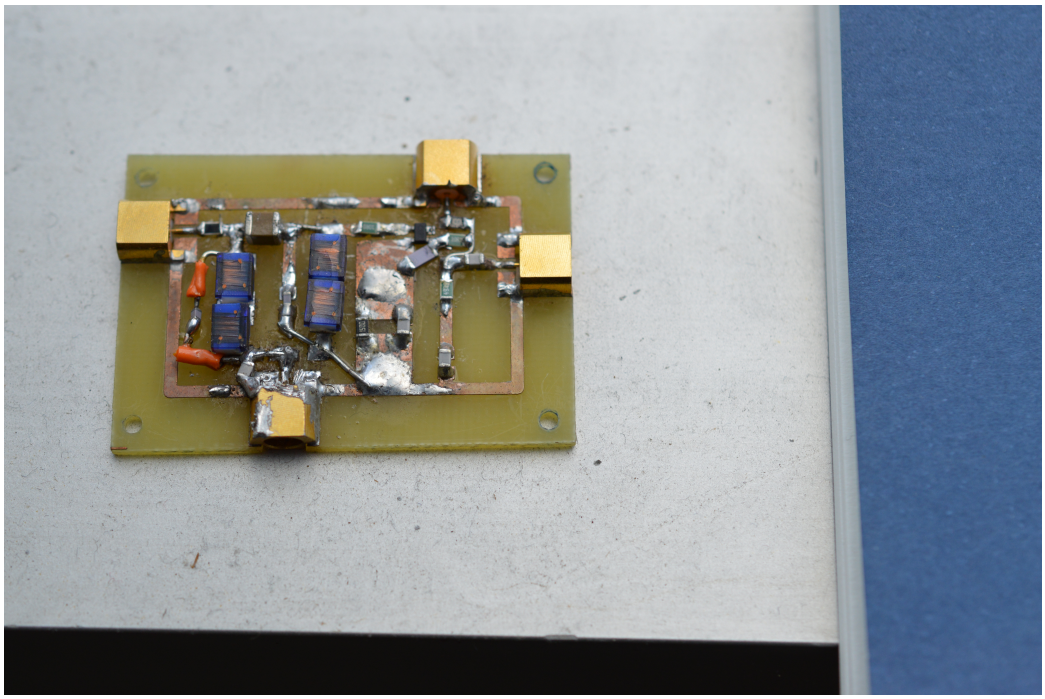

Figure C.2: *Picture of the double tank amplifier test circuit. A 50MΩ smd resistor was soldered in front of the first tank to simulate a tunnel jucntion.*

As can be seen from figure C.2, the double tank test setup was a bit rough. This is because we built it by modifying a single tank setup on a PCB that was only built for the single tank. Still, because our amplifier operates around 2.8MHz, this shouldn't be a problem.

References

[1] G. Binnig and H. Rohrer, *Scanning tunneling microscopy*, Surface Science **126**, 236 (1982).

[2] S. Loth, M. Etzkorn, C. P. Lutz, D. M. Eigler, and A. J. Heinrich, *Measurement of fast electron spin relaxation times with atomic resolution.*, Science **329**, 1628 (2010).

[3] H. Birk, M. J. M. De Jong, and C. Schönenberger, *Shot-noise suppression in the single-electron tunneling regime*, Physical Review Letters **75**, 1610 (1995).

[4] H. Birk, *Preamplifier for electric-current noise measurements at low temperatures*, Review of Scientific Instruments **67**, 2977 (1996).

[5] T. Martin and R. Landauer, *Wave-packet approach to noise in multichannel mesoscopic systems*, Physical Review B **45**, 1742 (1992).

[6] L. DiCarlo, Y. Zhang, D. T. McClure, C. M. Marcus, L. N. Pfeiffer, and K. W. West, *System for measuring auto- and cross correlation of current noise at low temperatures*, Review of Scientific Instruments **77**, 073906 (2006).

[7] T. Arakawa, Y. Nishihara, M. Maeda, S. Norimoto, and K. Kobayashi, *Cryogenic amplifier for shot noise measurement at 20 mK*, Applied Physics Letters **103**, 172104 (2013).